SUPPORTING INFORMATION FOR

Robust fossil evidence for Proboscidean frugivory and its lasting impact on South American ecosystems

Corresponding author. Erwin González Guarda

Email: erwin.gonzalez@uoh.cl

Supplementary Methods

Materials

Molars of Notiomastodon platensis

In this study, we used a comprehensive multi-proxy approach involving stable isotope analysis, dental microwear analysis, and analysis of microfossils from dental calculus of 96 *N. platensis* molars. This analysis integrated newly collected samples with previously published data[1, 2, 3].

The samples were procured from 40 sites, spanning latitudes between 31ºS and 36ºS (North–Central = Mediterranean climate) and between 38ºS and 42ºS (South–Central = Temperate climate). The chronological range of the selected specimens extends from approximately 30,000 to12,000 cal yr BP, covering the Pleistocene-Holocene transition. A complete compilation of the selected samples, along with their respective analyses, is provided in Dataset (Supplementary Data).

Stable isotope analysis. This analytical technique yields data pertinent to the dietary habits and trophic levels of the studied specimens. Additionally, it offers insights into environmental and climatic variability. For this study, stable isotope analysis was conducted on 24 new bioapatite samples extracted from dental enamel (Supplementary Data).

Dental microwear analysis. This technique offers insights into the dietary habits of mammals over the last days or weeks before their death, achieved through the examination of microscopic features on tooth enamel occlusal surfaces. Specifically, dental microwear sheds light into the available vegetation and habitat, as well as short-term dietary traits[4, 5]. In this study, we used 22 new samples (compared to the study by González-Guarda et al.[2]) for the analysis of dental microwear (Supplementary Table 6).

Analysis of microfossils from dental calculus. Plant micro remains found in dental calculus offer direct insights into an animal's diet[6] and can reflect long-term dietary patterns[7]. However, the specific timeframe represented by dental calculus is uncertain due to variable composition and formation processes among and within individuals[8].

Consequently, pinpointing the exact time particular plant micro remains were consumed is not possible[9]. Notably, older individuals present more microremains[8], suggesting that dental calculus may represent an average of multiple feeding events throughout an animal's life, assuming no calculus deposits are replaced or removed. Our study includes the analysis of 19 new samples from the occlusal surfaces of dental enamel (Supplementary Table 6)

Current samples

We examined eight *Pudu puda* samples from Rivers District (39°48′30″S 73°14′30″O) to determine their δ^{18}O values (Supplementary Table 3 and Supplementary

Data). The δ^{13}C values in *P. puda* were obtained from the data published by González-Guarda et al.[3] (Supplementary Table 3). Additionally, we collected modern plant samples (n = 237) from four locations (Supplementary Data): Tagua Tagua (34ºS), Fray Jorge National Park (30ºS), and Tantauco Park (43ºS). Our analysis also included δ^{13}C values of plants (from the Rivers District) published in González-Guarda et al.[3]

<u>*Methods*</u>

Stable isotopes analysis (*bioapatite*)

To obtain enamel samples, we used a rotary hand drill with a diamond-tipped dental burr, targeting as large an area as possible to mitigate the seasonal bias at the time of mineralization. Initially, molar surfaces were cleaned using a tungsten abrasive drill bit, followed by drilling with a diamond bit to remove enamel. Each fossil molar provided one sample band for oxygen and carbon isotope analysis. The powdered enamel samples, ranging from 3.5 mg to 9.5 mg, underwent chemical analyses at the Biomolecular Laboratory of the Institut Català de Paleoecologia Humana i Evolució Social (IPHES), following modified protocols from Koch et al.[10] and Tornero et al.[11].

This involved treating the samples with 0.1 M acetic acid [CH_3COOH] (0.1 ml solution/0.1 mg of sample) for four hours, neutralization with distilled water, and freeze-drying. Individual analyses of pretreated powders were conducted using a Thermo Kiel III device interfaced with a MAT Finnagan 253 at the Scientific and Technological Centers of the University of Barcelona (CCiTUB), Spain. The samples reacted in a vacuum with 100% phosphoric acid [H_3PO_4] at 70°C in individual vessels, followed by purification in an automated cryogenic distillation system. Measurement accuracy was ensured using two internal laboratory calcium carbonate standards (RC-1 and CECC) normalized to international standards NBS18 and NBS19.

A total of 16 RC-1 and CECC samples were measured (RC-1 expected values +2.83‰ for $\delta^{13}C$; CECC expected values −20.78‰ for $\delta^{13}C$). The mean analytical precision of RC-1 was +0.01‰ for $\delta^{13}C$ values and +0.01‰ for CECC. Stable isotope results follow the δ-notation $\delta^{H}X_{sample}=[(R_{sample}-R_{standard})/R_{standard}]x1000$, where X is the element, H is the mass of the rare, heavy isotope, and $R={}^{13}C/{}^{12}C$, or $^{18}O/^{16}O$. $\delta^{13}C$ and $\delta^{18}O$ values are expressed in the Vienna-Pee Dee Belemnite (VPDB) standard, and $\delta^{18}O$ also in terms of the VSMOW standard (Vienna Standard Mean Ocean Water), using the conversion formula: $\delta^{18}O_{SMOW} = (1.0309 \text{ x } \delta^{18}O_{VPDB}) + 30.909$.

For this study, we used $\delta^{13}C_{atmCO2} = -6.5‰$ because it is an accepted value for late Pleistocene studies[12]. Modern vegetation stable isotope data were corrected for the contemporary $^{13}C_{atmCO2}$ composition of −8‰[13]. An Estimated Consumed Plants (ECP) value for the mammals was derived from diet-to-tissue trophic discrimination studies [11], comparing it with sampled modern vegetation. We applied the equation $\mathcal{E}^{*} = 2.4 + 0.034$ (bm) to determine the enrichment between bioapatite and the diet of *P. puda* ($\mathcal{E}^{*}_{diet-bioapatite}$). Using the $\mathcal{E}^{*}_{diet-bioapatite}$ value of *P. puda's* ($\delta^{13}C = 12‰$), which is contingent on its body mass (9.6 kg), we enhanced the reliability of $\delta^{13}C_{bioapatite}$ comparisons across mammals of varying body masses[14]. For gomphotheres, we used an enrichment of 14.1‰ ($\mathcal{E}^{*}_{diet-bioapatite}$) [15, 16]. However, Acevedo et al.[17] used an enrichment of 15‰ ($\mathcal{E}^{*}_{diet-bioapatite}$) based on an estimated body mass of gomphotheres of 6,000 kg. Consequently, a multiproxy approach and consideration of isotopic proxy temporal resolution were necessary to reduce the uncertainty in enrichment values.

Stable isotopes analysis (*vegetation*)

Given the evidence suggesting that *N. platensis* primarily browsed in the North–Central region, we focused on sampling shrubs and trees across various environments between 30ºS and 43ºS. The plants were collected and pressed and later oven-dried at 50ºC in the laboratory. Analyses were conducted at the Laboratory for Biogeochemistry and Applied Stable Isotopes (LABASI) of the Departamento de Ecología, Pontificia Universidad Católica de Chile using a Thermo Delta V Advantage IRMS coupled with a Flash2000 Elemental Analyzer. To ensure consistency, cross-lab comparisons were conducted on identical samples, confirming reproducibility within the instruments' error margins (± 0.2%).

Analysis of microfossils from dental calculus

For calculus extraction, we first used dry cleaning to remove coarse sediment, followed by acetone cleaning to remove any remaining adhered sediment. The calculus was then carefully removed using a dental curette to collect small fragments, ensuring minimal damage to the enamel surface.

Microfossils were extracted from the calculus samples using the chemical processing method described by Wesolowski et al.[18]. To quantify microfossils in dental calculus, a *Lycopodium* tablet was added to each sample. We then applied a 10% hydrochloric acid solution to fully dissolve the carbonates. Following dissolution, the samples were centrifuged at 1000 RPM for 5 min, and the supernatant was discarded.

The samples were then washed with distilled water and centrifuged again. After the final centrifugation, the distilled water was replaced with 96% ethanol.

For microscopic examination, three slides per sample were prepared using Entellan ® and analyzed under a polarized light microscope with 400x and 630x magnification. All microfossils, including phytoliths, starch granules, charcoal, and Lycopodium spores, were counted and recorded. We employed Maher's[19] method as modified by Wesolowski et al.[20], to calculate microfossil concentration.

Dental microwear analysis.

Microphotographs were captured with a Blackfly S digital camera and the Kivy Mic Capture Z software. We used the Helicon Focus 7 software to merge images from different focal planes for a greater depth of field and used ImageJ to add scale bars. To minimize inter-observer error, all specimens were analyzed by two independent observers (IRP and FR).

Supplementary Results

Preservation of the isotopic signal in N. platensis

The samples analyzed in this study showed an average $\Delta^{18}O_{CO3-PO4}$ value of approximately 9.0‰, aligning with the standard $\Delta^{18}O_{CO3-PO4}$ range for unaltered bioapatite of present-day mammals (i.e., 8.6 – 9.1‰)[21]. This alignment indicates the preservation of original $\delta^{18}O_{CO3}$ and $\delta^{18}O_{PO4}$ values. The observed high correlation coefficient between these isotopic values ($R = 0.9$, $p < 0.001$) supports the hypothesis that CO_3^{-2} and PO_4^{-3} components in bioapatite are cogenetic precipitated in equilibrium from body water occurring under the relatively invariant mammalian body temperatures.

Supplementary Discussion

The objective of our study was to present robust evidence of the neotropical anachronism hypothesis of Janzen and Martin[22] and, consequently, the risk of extinction of megafaunal fruit plants from Central Chile. Although our evidence is robust, we discuss the paleoenvironmental and paleoclimatic context in which the discovery could have occurred.

The finding of frugivory, combined with $\delta^{13}C_{enamel}$ values, suggests a large standing biomass of shrubs or trees in central Chile during the late Pleistocene (Fig. 2)[3]. This finding is consistent with pollen records from north-central[23, 24], and south-central Chile[25]. This correlation supports the hypothesis that the diet of South American gomphotheres, such as *N. platensis*, was more influenced by resource availability than by their potential dietary range [26, 27, 2, 28, 29]. The presence of woody vegetation (resource availability) in central Chile can likely be attributed to the moisture-retaining Andes and Coastal Range and the Pacific Ocean's thermoregulatory effects[30]. These environmental factors may have facilitated a solid ecological link between woody vegetation and *N. platensis*, increasing the likelihood of recording frugivory in central Chile. This hypothesis also offers a plausible explanation for the lack of evidence for frugivory in other regions of South America since most of the environments where gomphothere fossils have been recorded are open or semi-open[2, 16].

Therefore, the evidence consistently suggests that gomphotheres were frugivorous under a primarily forested environment. Notably, the discovery of dental calculus evidence of frugivory involving a megafaunal fruit (*Jubaea chilensis*) – currently outside its distribution range – challenges the expected range contraction of a thermophilic species during Pleistocene glaciations. However, frugivory could also represent isolated events, particularly given the presumed hyper-cold and humid late Pleistocene paleoenvironment of central Chile[3,4], which seemingly would not favor megafaunal plant presence, apart from glacial relicts.

Thus, we conducted stable isotopic analyses on both fossils and contemporary plants to determine if the paleoenvironment was conducive to frugivory in *N. platensis*.

Our stable isotope results ($\delta^{18}O_{meteoric\ water}$ and $\delta^{13}C_{enamel}$; Supplementary Table 3) from *N. platensis*, alongside the modern vegetation baselines ($\delta^{13}C_{modern\ vegetation}$) from central Chile (Supplementary Table 2), indicate significant environmental variability (Fig. 2), differing from the previously interpreted cold and wet conditions (i.e., conditions akin to Valdivian rainforest or open montane forest in the lowlands) (Supplementary Table 1; Fig. 1). These findings suggest that the landscape inhabited by *N. platensis* was likely suitable for this biogeographic expansion of megafaunal plants.

Our interpretations are corroborated by two recent multiproxy studies of the sediments of the ancient Tagua Tagua lake (34ºS), such as lipid biomarkers that indicated more arid environments[31] and the phytoliths of the palm *J. chilensis* indicated warmer environments[32]. Both studies conclude that the paleoenvironment and paleoclimate of north-central Chile were much drier and warmer than previously established. Nonetheless, the extent of Mediterranean sclerophyllous vegetation in north-central Chile at the end of the Pleistocene is still largely unknown, leaving the role of proboscideans as dispersers of present-day sclerophyllous tree species (many of which lack fleshy fruits) uncertain.

Consequently, the finding of frugivory not only proves an ecological hypothesis but will likely have implications in paleoenvironmental and paleoclimatic reconstruction studies of the Southern cone region of South America.

FIGURES

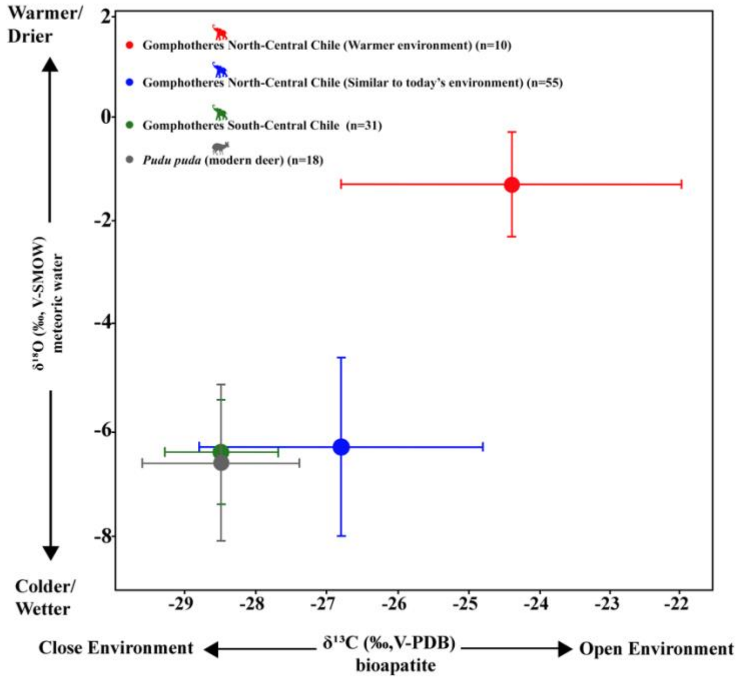

Supplementary Fig. 1 Graphical results of isotopic analyses derived from multiple sources showing the mean values of δ^{13}Cbioapatite (‰, V-PDB) and δ^{18}Ometeoric water (‰, V-SMOW) for *Notiomastodon platensis* and *Pudu puda*.

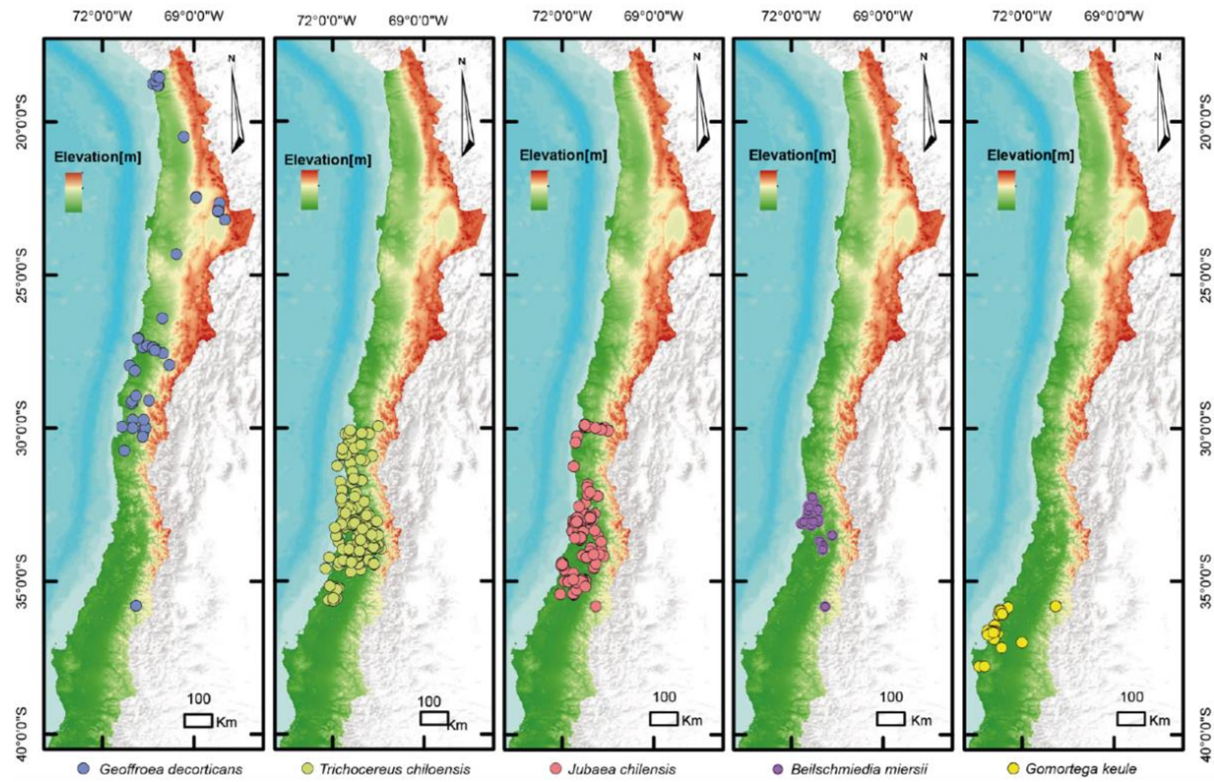

Supplementary Fig. 2 Distribution of plants with fleshy fruits in Central Chile.

TABLES

Supplementary Table 1. Summary data of $\delta^{13}C_{VPDB}$ values in dental enamel bioapatite.

Latitude	N	$\delta^{13}C$ (‰, V-PDB)				piC3				piC4				Niche breadth (BA)			
		Min	Max	Mean	SD	Min	Max	Mean	SD	Min	Max	Mean	SD	Min	Max	Mean	SD
North-Central (31°– 36°S)	64	-15.02	-3.99	-11.40	2.17	0.43	1.00	0.93	0.13	0.00	0.57	0.07	0.13	0.00	0.98	0.16	0.26
South-Central (38°– 42°S)	30	-15.23	-11.17	-13.31	0.82	0.98	1.00	1.00	0.00	0.00	0.02	0.00	0.00	0.00	0.04	0.00	0.01

Note: Proportional contributions of diet sources (piC3 and piC4 plants) and standardized isotopic niche breadth (BA) of *Notiomastodon platensis* from central Chile.

Supplementary Table 2. Summary of stable isotope data ($\delta^{13}C$, ‰V-PDB) of the modern sample plants collected in central Chile.

$\delta^{13}C$ (‰V-PDB)					
Sites	**n**	**Max**	**Min**	**Mean**	**(σ)**
Fray Jorge National Park (Hygrophilous forest) (30º 30′ S, 71º 35′ W) (wetter area). 1000 mm/yr. 13.7 ºC	43	-26	-3	-3	2
Fray Jorge National Park (Semi-arid scrub) (30º 30′ S, 71º 35′ W) (arid area) 147 mm/yr. 13.7 ºC.	56	21	-31	-26	3
Tagua Tagua (Sclerophyllous forest) (34° 33' S, 71º 9' W) (wetter area). 800 mm/yr. 15 ºC.	60	-24	-33	-29	2
Tagua Tagua (Sclerophyllous forest) (34º 30' S, 71º 1' W) (more arid area). 800 mm/yr. 15 ºC.	33	-23	-2	-25	1
Tantauco Park (Temperate Rain forest) (43° 12′ S, 74º 11′ W) (wetter area). 3000 mm/yr. 10 ºC.	45	-26	-34	-31	2

Note: Number of samples (n), maximum (Max), minimum (Min), mean values and standard deviation (σ). All raw data presented in this table are normalized based on pre-industrial atmospheric conditions ($\delta^{13}C_{atmCO2}$= -6.5‰).

Supplementary Table 3. Summary of stable isotope data of the $\delta^{18}O_{meteoric\ water}$ (‰V-SMOW) values.

$\delta^{18}O$ (‰V-SMOW)					
Sites	**n**	**Max**	**Min**	**Mean**	**(σ)**
North-Central (warmer environment)	10	0.5	-3	-1.8	1
North-Central (environmental conditions similar to the present)	54	-3	-15	-6.5	2
South-Central (environmental conditions similar to the present)	31	-4	-9	-6.9	1
Pudu puda (current deer)	8	-3.6	-8.2	-6.6	1.5

Note: The values were calculated from $\delta^{18}O_{CO3}$ (‰, V-PDB) values of *Notiomastodon platensis* and *Pudu puda* (current deer). Our analysis was based on the $\delta^{18}O$ values published in González-Guarda et al., (2018) and unpublished values presented in this study. Number of samples (n), maximum (Max), minimum (Min), mean values and standard deviation (σ).

Supplementary Table 4. Concentration of starch, sclereids and phytoliths, expressed in microfossil per gram (mf/g) of dental calculus.

Sample	Locality	Reserve Starch (mf/g)	Transitory Starch (mf/g)	Sclereids (mf/g)	Raphids (mf/g)	References
PV267A	Quereo (31ºS)	152711	0	0	0	This study
PV264	Quereo (31ºS)	0	0	1587	0	This study
PV235	Catapilco (33ºS)	4820	0	2410	0	This study
QUI1	Quilpué (33ºS)	4698	9396	0	0	This study
QUI2	Quilpué (33ºS)	14094	0	0	0	This study
MHNV1	Casablanca (33ºS)	11100	2048	0	342	This study
RMPL05	El Noviciado (33ºS)	514	5820	0	0	This study

Sample	Locality	Reserve Starch (mf/g)	Transitory Starch (mf/g)	Sclereids (mf/g)	Raphids (mf/g)	References
354A	Algarrobo (33ºS)	422	0	0	0	This study
PV22	Lagunillas	1922	0	0	0	This study
PV1E	Tagua Tagua (34ºS)	5741	0	0	0	This study
PV47A	Tagua Tagua (34ºS)	799508	0	0	0	This study
PV47B	Tagua Tagua (34ºS)	992682	0	198536	0	This study
PV47C	Tagua Tagua (34ºS)	55918	0	0	0	This study
PV47F	Tagua Tagua (34ºS)	6532	0	129	0	This study
PV47G	Tagua Tagua (34ºS)	2819	0	0	0	This study
PV47K	Tagua Tagua (34ºS)	1638	0	0	0	This study
PV49	Tagua Tagua (34ºS)	3381	0	0	0	This study
TT1	Tagua Tagua (34ºS)	0	23339	0	0	This study
PV15	Parral (36ºS)	0	0	0	62367	This study
PV19	Parral (36ºS)	9287	0	0	0	This study
PV55	Parral (36ºS)	42342	0	0	0	This study
TR1	El Trébol (39ºS)	299	0	0	0	This study
CHO01	Choroico (40ºS)	142	0	0	0	This study
LP15	La Plata (40ºS)	890	0	445	0	This study
LP16	La Plata (40ºS)	910	0	0	0	This study
PV44	Río Bueno (40ºS)	4306	0	0	0	This study
PI14	Pilauco (40ºS)	0	0	1344	0	This study

Supplementary Table 5. Percentages of the types of diet assigned to each molar studied by analyzing the microfossils of the dental calculus.

(B = browser diet; M = mixed diet).

Code	Site	% HH	% AA	Diet	References
PV40	Illapel	0.0%	100.0%	B	González-Guarda et al., (2018)
PV267a	Quereo	5.2%	94.8%	B	González-Guarda et al., (2018)
PV264	Quereo	15.6%	84.4%	B	This study
PV235	Catapilco	31.3%	68.8%	B	This study
QUI1	Quilpue	19.4%	80.6%	B	This study
QUI2	Quilpue	8.3%	91.7%	B	This study
MHNV1	Casablanca	73.3%	26.7%	B	González-Guarda et al., (2018)
RMPL05	Noviciado	5.3%	94.7%	B	This study
354a	El Quisco	21.6%	78.4%	B	González-Guarda et al., (2018)
354b	El Quisco	18.8%	81.3%	B	González-Guarda et al., (2018)
PV22	Lagunillas	55.2%	44.8%	B	González-Guarda et al., (2018)
1637	Navidad	20.0%	80.0%	B	González-Guarda et al., (2018)
PV45	Tagua-Tagua	0.0%	100.0%	B	González-Guarda et al., (2018)
PV1E	Tagua-Tagua	5.0%	95.0%	B	This study
PV256	Tagua-Tagua	2.5%	97.5%	B	González-Guarda et al., (2018)
PV47a	Tagua-Tagua	18.2%	81.8%	B	González-Guarda et al., (2018)
PV47b	Tagua-Tagua	23.8%	76.2%	B	González-Guarda et al., (2018)
PV47C	Tagua-Tagua	52.0%	48.0%	M	González-Guarda et al., (2018)
PV47F	Tagua-Tagua	33.3%	66.7%	B	González-Guarda et al., (2018)
PV47G	Tagua-Tagua	33.3%	66.7%	B	González-Guarda et al., (2018)
PV47H	Tagua-Tagua	5.8%	94.2%	B	González-Guarda et al., (2018)
PV47I	Tagua-Tagua	0.0%	100.0%	B	González-Guarda et al., (2018)

Code	Site	% HH	% AA	Diet	References
PV47J	Tagua-Tagua	29.6%	70.4%	B	González-Guarda et al., (2018)
PV47K	Tagua-Tagua	8.7%	91.3%	B	González-Guarda et al., (2018)
PV47L	Tagua-Tagua	0.0%	100.0%	B	González-Guarda et al., (2018)
PV49	Tagua-Tagua	25.6%	74.4%	B	This study
TT1	Tagua-Tagua	33.0%	67.0%	B	This study
PV15	Parral	19.0%	81.0%	B	This study
PV19	Parral	2.2%	97.8%	B	This study
PV55	Parral	2.9%	97.1%	B	This study
CHA01	Chan-Chan	0.0%	100.0%	B	González-Guarda et al., (2018)
TR1	El Trébol	62.8%	37.2%	B	González-Guarda et al., (2018)
TR18	El Trébol	18.5%	81.5%	B	González-Guarda et al., (2018)
CHO01	Choroico	69.4%	30.6%	B	González-Guarda et al., (2018)
LP13	La Plata	43.7%	56.3%	B	González-Guarda et al., (2018)
LP14	La Plata	37.6%	62.4%	B	González-Guarda et al., (2018)
LP15	La Plata	17.4%	82.6%	B	González-Guarda et al., (2018)
LP16	La Plata	16.7%	83.3%	B	González-Guarda et al., (2018)
PV44	Río Bueno	11.0%	89.0%	B	González-Guarda et al., (2018)
PV43	San Pablo	10.2%	89.8%	B	González-Guarda et al., (2018)
PI14	Pilauco	9.8%	90.2%	B	González-Guarda et al., (2022)
LN8	Los Notros	63.1%	36.9%	M	González-Guarda et al., (2022)
CHI1	Chiloé	0.0%	100.0%	B	González-Guarda et al., (2022)
CHI2	Chiloé	15.5%	84.5%	B	González-Guarda et al., (2022)

Supplementary Table 6. Results of the analysis of dental microwear in *Notiomastodon platensis* from central Chile.

Taxon	n	NS	SD	NP	SD	%PP	%G	SWS	%LP	%XS
Extinct *N. platensis*	19	13.9	6	21.7	9.2	89.4	73.6	2	84.2	68.4
Extant *L. africana*	33	17.4	5.3	22.9	3.9	0.5	36.4	2.8	54.6	3
Extant *L. cyclotis*	6	12.9	5.1	29.8	4	33.3	33.3	3.1	50	66.7
Extant *E. maximus*	10	18.3	4.3	20.9	3	0	50	3.1	70	80

Note: Number of samples (n); number of scratches (NS); standard deviation (SD); number of pits (NP); puncture pits (PP); gouges (G); scratch width (SWS); large pits (LP); percentage of specimens with cross scratches (XS).

References

1. González-Guarda E, *et al.* Late Pleistocene ecological, environmental and climatic reconstruction based on megafauna stable isotopes from northwestern Chilean Patagonia. *Quaternary Science Reviews* **170**, 188-202 (2017).

2. González-Guarda E, *et al.* Multiproxy evidence for leaf-browsing and closed habitats in extinct proboscideans (Mammalia, Proboscidea) from Central Chile. *Proceedings of the National Academy of Sciences* **115**, 9258-9263 (2018).

3. González-Guarda E, *et al.* Dietary ecological traits of extinct mammalian herbivores from the last glacial termination at the Pilauco Site, Chile. *Quaternary Research* **109**, 141-156 (2022).

4. Grine FE. Dental evidence for dietary differences in *Australopithecus* and *Paranthropus*: a quantitative analysis of permanent molar microwear. *Journal of human evolution* **15**, 783-822 (1986).

5. Semprebon GM, Rivals F, Solounias N, Hulbert Jr RC. Paleodietary reconstruction of fossil horses from the Eocene through Pleistocene of North America. *Palaeogeography, Palaeoclimatology, Palaeoecology* **442**, 110-127 (2016).

6. Cordova C, Avery G. African savanna elephants and their vegetation associations in the Cape Region, South Africa: Opal phytoliths from dental calculus on prehistoric, historic and reserve elephants. *Quaternary International* **443**, 189-211 (2017).

7. Weyrich LS, *et al.* Neanderthal behaviour, diet, and disease inferred from ancient DNA in dental calculus. *Nature* **544**, 357-361 (2017).

8. Power RC, Salazar-García DC, Wittig RM, Freiberg M, Henry AG. Dental calculus evidence of Taï Forest Chimpanzee plant consumption and life history transitions. *Scientific Reports* **5**, 15161 (2015).

9. Weber S, Price MD. What the pig ate: A microbotanical study of pig dental calculus from 10th–3rd millennium BC northern Mesopotamia. *Journal of Archaeological Science: Reports* **6**, 819-827 (2016).

10. Koch PL, Tuross N, Fogel ML. The effects of sample treatment and diagenesis on the isotopic integrity of carbonate in biogenic hydroxylapatite. *Journal of Archaeological Science* **24**, 417-429 (1997).

11. Koch PL. Isotopic study of the biology of modern and fossil vertebrates. *Stable isotopes in ecology and environmental science*, 99-154 (2007).

12. Tipple BJ, Meyers SR, Pagani M. Carbon isotope ratio of Cenozoic CO2: A comparative evaluation of available geochemical proxies. *Paleoceanography* **25**, (2010).

13. Marino BD, McElroy MB. Isotopic composition of atmospheric CO2 inferred from carbon in C4 plant cellulose. *Nature* **349**, 127-131 (1991).

14. Tejada-Lara JV, MacFadden BJ, Bermudez L, Rojas G, Salas-Gismondi R, Flynn JJ. Body mass predicts isotope enrichment in herbivorous mammals. *Proceedings of the Royal Society B* **285**, 20181020 (2018).

15. Cerling TE, Harris JM. Carbon isotope fractionation between diet and bioapatite in ungulate mammals and implications for ecological and paleoecological studies. *Oecologia* **120**, 347-363 (1999).

16. Domingo L, Prado JL, Alberdi MT. The effect of paleoecology and paleobiogeography on stable isotopes of Quaternary mammals from South America. *Quaternary Science Reviews* **55**, 103-113 (2012).

17. Asevedo L*, et al.* Isotopic paleoecology (δ13C, δ18O) of late Quaternary herbivorous mammal assemblages from southwestern Amazon. *Quaternary Science Reviews* **251**, 106700 (2021).

18. Wesolowski V, de Souza SMFM, Reinhard K, Ceccantini G. Grânulos de amido e fitólitos em cálculos dentários humanos: contribuição ao estudo do modo de vida e subsistência de grupos sambaquianos do litoral sul do Brasil. *Revista do Museu de Arqueologia e Etnologia*, 191-210 (2007).

19. Maher Jr LJ. Statistics for microfossil concentration measurements employing samples spiked with marker grains. *Review of Palaeobotany and Palynology* **32**, 153-191 (1981).

20. Wesolowski V, de Souza SMFM, Reinhard KJ, Ceccantini G. Evaluating microfossil content of dental calculus from Brazilian sambaquis. *Journal of Archaeological Science* **37**, 1326-1338 (2010).

21. Iacumin P, Bocherens H, Mariotti A, Longinelli A. Oxygen isotope analyses of co-existing carbonate and phosphate in biogenic apatite: a way to monitor diagenetic alteration of bone phosphate? *Earth and Planetary Science Letters* **142**, 1-6 (1996).

22. Janzen DH, Martin PS. Neotropical anachronisms: the fruits the gomphotheres ate. *Science* **215**, 19-27 (1982).

23. Heusser CJ. Quaternary pollen record from laguna de Tagua Tagua, Chile. *Science* **219**, 1429-1432 (1983).

24. Valero‐Garcés BL*, et al.* Palaeohydrology of Laguna de Tagua Tagua (34 30 ′ S) and moisture fluctuations in Central Chile for the last 46 000 yr.

Journal of Quaternary Science: Published for the Quaternary Research Association **20**, 625-641 (2005).

25. Moreno PI, Denton GH, Moreno H, Lowell TV, Putnam AE, Kaplan MR. Radiocarbon chronology of the last glacial maximum and its termination in northwestern Patagonia. *Quaternary Science Reviews* **122**, 233-249 (2015).

26. Asevedo L, D'Apolito C, Misumi SY, de Barros MA, Barth OM, dos Santos Avilla L. Palynological analysis of dental calculus from Pleistocene proboscideans of southern Brazil: A new approach for paleodiet and paleoenvironmental reconstructions. *Palaeogeography, Palaeoclimatology, Palaeoecology* **540**, 109523 (2020).

27. Dantas MAT, Liparini A, Asevedo L, de Melo França L, Cherkinsky A. Annual isotopic diet (δ13C, δ18O) of *Notiomastodon platensis* (Ameghino, 1888) from Brazilian Intertropical Region. *Quaternary International* **610**, 38-43 (2022).

28. Rivals F, Semprebon GM, Lister AM. Feeding traits and dietary variation in Pleistocene proboscideans: A tooth microwear review. *Quaternary Science Reviews* **219**, 145-153 (2019).

29. Araújo T, Machado H, Mothé D, dos Santos Avilla L. Species distribution modeling reveals the ecological niche of extinct megafauna from South America. *Quaternary Research* **104**, 151-158 (2021).

30. Villagrán Moraga C, Hinojosa Opazo L. Esquema biogeográfico de Chile. (2005).

31. Frugone Álvarez M*, et al.* Climate changes inferred from sedimentary biomarkers during the Pleistocene-Holocene transition in central Chile (~34ºS). In: *XXI INQUA Meeting*) (2023).

32. Godoy-Aguirre C.*, et al.* First evidence of plant use in Tagua Tagua 3, a Late Pleistocene site in central Chile: Cultural and environmental implications. In: *XXI INQUA Meeting*) (2023).